

# Fast spinning neutron stars: unified equations of state, crust effects, maximum rotating configurations

**A. Li**

Department of Astronomy, Xiamen University, Xiamen, Fujian 361005, China

E-mail: liang@xmu.edu.cn

**N. B. Zhang, B. Qi**

Shandong Provincial Key Laboratory of Optical Astronomy and Solar-Terrestrial Environment, Institute of Space Sciences, Shandong University, Weihai 264209, China

**G. F. Burgio**

INFN, Sezione di Catania, Via Santa Sofia 64, I-95123 Catania, Italy

**Abstract.** We study the crust effects on fast-rotating configurations of neutron stars (NSs). For this aim, we employ four unified equations of state (EoS) for both the cores and crusts, namely BCPM, BSk20, BSk21, Shen-TM1, as well as two non-unified EoS widely used in the literature, i.e. APR and GM1 EoS. All the core EoSs satisfy the recent observational constraints of the two massive pulsars whose masses are precisely measured. We show that the NS mass-equatorial radius relations are slightly affected by the smoothness at the core-crust matching interface. However, the uncertainties in the crust EoS and the matching interface bring insignificant changes, even at maximally rotating (Keplerian) configurations. For all four unified EoS, rotations can increase the star's gravitational mass up to 18%–19% and the equatorial radius by 29%–36%. For stars as heavy as  $1.4 M_{\odot}$ , the radius increase is more pronounced, reaching 41%–43%, i.e. 5–6 km. Moreover, by comparing the present calculations with recent simultaneous determinations of mass and radius for two X-ray bursts, 4U 1608-52 and 4U 1724-307, we propose that they might be rapidly spinning NSs, in order to account for their measured large radii.

*Keywords:* neutron stars, equation of state, fast rotating

## 1. Introduction

Neutron stars (NSs) are by far one of the most interesting observational objects, since many mysteries remain on them due to their complexity. Future observations with advanced telescopes such as SKA, Advanced LIGO and VIRGO, AXTAR [1], FAST [2],

NICER [3], LOFT [4], and eXTP [5], will hopefully provide precise measurements of their mass and/or radius, thus improving our current knowledge of such stellar objects. Those observations would also serve as a valuable guidance for improving models of such matter. Theoretically, a wide range of matter density from  $\sim 0.1 \text{ g cm}^{-3}$  in the star atmosphere, to values larger than  $\sim 10^{14} \text{ g cm}^{-3}$  in the star core, is encountered in those objects. At the moment the various model calculations, based on different theoretical frameworks, give distinct results especially for the high-density inner crust and core regions. Accumulating observational studies might suffer from atmosphere modelling, burst cooling modelling and systematic data errors (see, e.g., [6, 7]). Therefore, for the study of NSs, particular attention should be paid on combining realistic enough theoretical models with accumulated NS observations. The present work is along this line.

Recently the importance of a unified EoS for the wide range of baryonic densities in a NS has been recognized (see, e.g., [8, 9, 10, 11]). It may be necessary to calculate all EoS segments (outer crust, inner crust, liquid core) using the same nuclear interaction, since matching problems in non-unified EoS could bring nontrivial conflicts on the predictions of the stars' radii (see, e.g., [8, 12]). The corresponding effects may be more important for distorted fast-rotating stars than for static ones (see, e.g., [13, 14]). We examine in detail such problems in the present work.

The observations of massive NSs [15, 16, 17] have already ruled out soft NS EoS which cannot reach  $2 M_{\odot}$  maximum mass. This serves here as a criterion for our selection of NS (core) EoS. The calculations are mainly done for four available unified EoS, namely BCPM [18], BSk20, BSk21 [19], Shen-TM1 [20]. For comparison, we also use the non-unified APR [21] and GM1 [22] EoS for the core, with the Baym-Pethick-Sutherland (BPS) [23] and the Negele-Vautherin (NV) [24] EoS for the outer and the inner crust, respectively.

The BCPM EoS, named after Barcelona-Catania-Paris-Madrid energy density functional [18], is based on the microscopic Brueckner-Hartree-Fock (BHF) theory [25]. The BSk20 EoS belongs to the family of Skyrme nuclear effective forces derived by the Brussels-Montreal group [19]. The high-density part of the BSk20 EoS is adjusted to fit the result of the APR [21] EoS. The Shen-TM1 EoS [20] is based on a phenomenological nuclear relativistic mean field (RMF) model with TM1 parameter set. The GM1 core EoS is from RMF calculation with GM1 parameter set [22]. The BPS outer crust EoS [23] is based on a semiempirical mass formula for matter from  $10^7 \text{ g cm}^{-3}$  to  $3.4 \times 10^{11} \text{ g cm}^{-3}$ . The NV inner crust EoS [24] is from quantal Hartree-Fock calculations of spherical Wigner-Seitz cells.

In a previous study [8], the authors concluded that the uncertainties of non-unified EoS arise from unlike saturation properties and density dependence of the symmetry energies for the two matching models. As we will see later, the results are also dependent on the smoothness at the matching interface.

In addition, we are also interested in how fast a NS can rotate, and its maximum frequency, since very useful informations can be drawn from the spin frequency

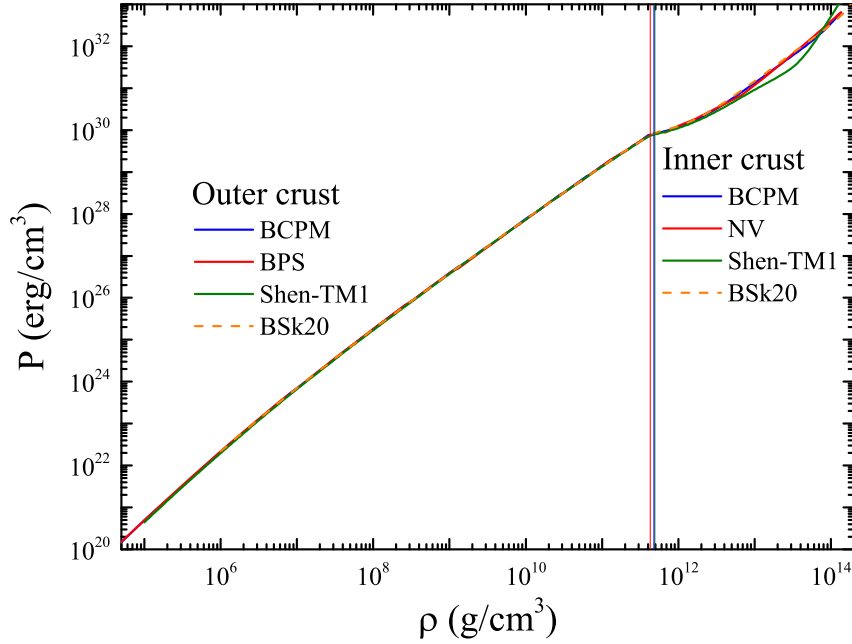


**Figure 1.** (Color online) Various EoS for both outer crust and inner crust employed in the present work. Among them, BCPM, Shen-TM1, BSk20 are three unified NS EoS.

observations of a star, such as its possible evolution process (see, e.g., [26]), inner composition (quarks confined or not) (see, e.g., [10, 27, 28, 29, 30, 31, 32, 33, 34, 35, 36]), potential central engine for short Gamma Ray Burst (SGRBs) (see, e.g., [11]), etc. For this purpose, the maximally possible frequency, namely the Keplerian frequency, is calculated for the four unified EoSs, as well as the corresponding stars' configurations. In particular, we relate our calculations to recent observations from two low-mass X-ray binaries, i.e. a photospheric radius expansion (PRE) burst in 4U 1724-307 [37] and a X-ray buster in 4U 1608-52 [38]. It was suggested by the authors that high spin frequencies may be present, using the cooling tail method with burst data [6]. Our results are consistent with their conclusions, i.e. the large observed radii may be due to the flattening of the fast rotating object.

The paper is organized as follows. We provide a short overview of the theoretical frameworks and discussions of our results in Sect. 2, before drawing conclusions in Sect. 3.

## 2. Results and discussion

Theoretically, global properties like mass, radius, spin period of NSs are studied by using the overall EoSs as basic input, and ignoring their thin atmosphere ( $\sim 0.1 - 10$ ) cm, where hot X-ray originates. In the outer crust, at densities below  $\sim 10^7$  g cm $^{-3}$ , nuclei

**Table 1.** EoS data at various crust-core matching interfaces used for the study of the crust effects. The unified BCPM EoS data are taken from Ref. [18]. The number density  $n$  is in  $\text{fm}^{-3}$ , the energy density  $\rho$  is in  $10^{14} \text{ g cm}^{-3}$ , and the pressure  $P$  is in  $10^{33} \text{ erg cm}^{-3}$ .

	inner crust			core			
	BCPM	NV	Shen-TM1	BCPM	APR	Shen-TM1	GM1
$n$	0.08	0.08	0.0797	0.0825	0.09	0.0821	0.0918
$\rho$	1.3518	1.3522	1.3429	1.394	1.5197	1.3843	1.5473
$P$	0.6355	0.6503	1.2136	0.6916	0.9282	1.3288	1.3295

arrange themselves in a Coulomb lattice mainly populated by  $^{56}\text{Fe}$  nuclei. At higher densities ( $10^7 \text{ g cm}^{-3} - 4 \times 10^{11} \text{ g cm}^{-3}$ ) the nuclei are stabilized against  $\beta$ -decay by the filled Fermi sea of electrons, and become increasingly neutron-rich. The composition of the outer crust is mainly determined by the nuclear masses, which are experimentally measured close to stability, whereas the masses of very neutron-rich nuclei are not known, and they have to be calculated using nuclear models. The inner crust is a non-uniform system of more exotic neutron-rich nuclei, degenerate electrons and superfluid neutrons. The density range extends from  $4 \times 10^{11} \text{ g cm}^{-3}$  to  $\sim 10^{14} \text{ g cm}^{-3}$ , at which nuclei begin to dissolve and merge together. Non-spherical shapes of nuclear structures, generically known as nuclear “pasta”, may appear at the bottom layers of the inner crust. Actually, one of NSs’ irregular behaviours, *glitch*, is closely related to the inner crust EoS and the crust-core transition properties, see (see, e.g., [10, 11, 39, 40, 41, 42, 43]).

In Fig. 1 we show both the outer and inner crust EoS for the different theoretical approaches discussed above. We observe that the outer crust EoSs, displayed left the vertical lines, differ by a little one from each other. On the other hand, due to different treatments for the neutron gas and some complicated nuclear shapes, uncertainties are still present in the EoS of the inner crust, which exhibits some differences. In Fig. 2, we show the EoS for the inner crust (below the vertical lines) and the core (above the vertical line). Plus signs indicate the transition point from the inner crust to the core for each chosen EoS. Detailed EoS data at various crust-core matching interfaces are collected in Table 1, where the matching is done so that the pressure is an increasing function of the energy density. We notice that the matching of GM1 core (dotted black) to Shen-TM1 crust (solid green) shows an evident non-smooth behaviour for the  $dP/d\rho$  (or  $dP/dn$ ) slope, compared to the matching to BCPM and NV crust. We will study more in detail the corresponding effects.

The strongest uncertainty concerns the dense core part ( $> 10^{14} \text{ g cm}^{-3}$ ), which is mainly composed by uniform nuclear matter in  $\beta$ -equilibrium with leptons. The determination of the EoS represents the main problem, also because first principle QCD calculations are difficult to perform in such a many-body system. Moreover, since in most of the model calculations available in the literature, a central density as high as 7 – 10 times the nuclear saturation density ( $\rho_0 = 2.7 \times 10^{14} \text{ g cm}^{-3}$ ) is found for the maximum mass, one or more types of strangeness phase transitions may

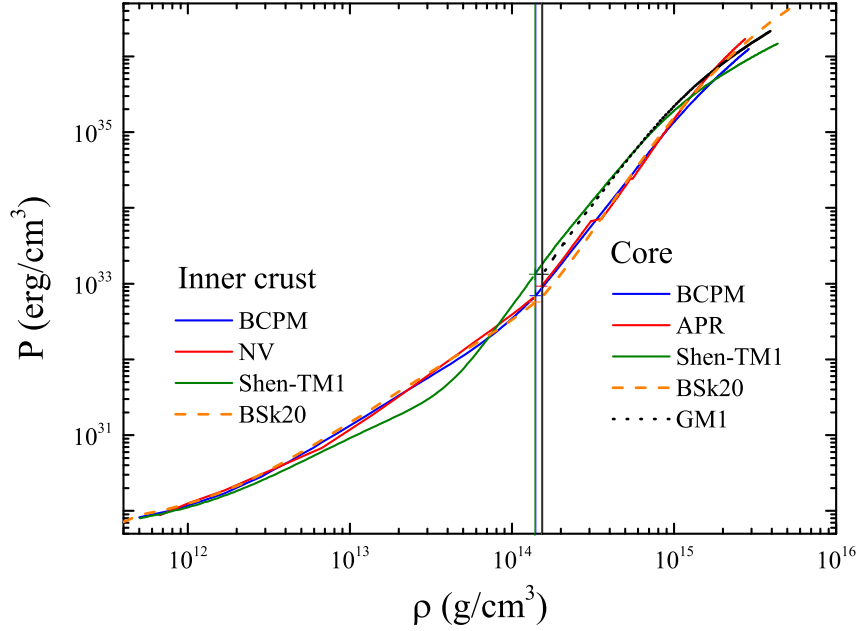


**Figure 2.** (Color online) Same with Fig. 1, but for both inner crust and core. Plus signs label the beginning of core EoS. Saturation properties of four core EoS (BCPM, APR, Shen-TM1, and GM1) are presented in Table 2, along with the empirical ranges also listed in the last row.

**Table 2.** Properties of nuclear matter at saturation predicted by four core EoS employed in this study, in comparison with the empirical ranges. The number density  $n_0$  is in  $\text{fm}^{-3}$ . The energy per baryon  $E/A$  and the compressibility  $K$  are in MeV, as well as the symmetry energy  $E_{\text{sym}}$  and its slope  $L$  at saturation.

EoS	$n_0$ ( $\text{fm}^{-3}$ )	$E/A$ (MeV)	$K$ (MeV)	$E_{\text{sym}}$ (MeV)	$L$ (MeV)
BCPM	0.16	-16.00	213.75	31.92	52.96
APR	0.16	-16.00	247.3	33.9	53.8
Shen-TM1	0.145	-16.26	281.14	36.89	110.79
GM1	0.153	-16.32	299.2	32.4	93.9
Empirical	$0.16 \pm 0.01$	$-16.0 \pm 0.1$	$220 \pm 30$	$31 \pm 2$	$\sim 60 \pm 25$

take place in the NSs' innermost parts, for example, hyperons (see, e.g., [44, 45]), kaon meson condensation (see, e.g., [46, 47, 48]), Delta excitation (see, e.g., [49]), quark deconfinement (see, e.g., [50, 51]). Due to our poor knowledge of the strange baryonic interaction and/or quark interaction, we restrict ourselves to normal nuclear matter, leaving the effects from possible strangeness phase transitions to a future study.

In Table 2 we display the main features of our selected EoS at the saturation point.

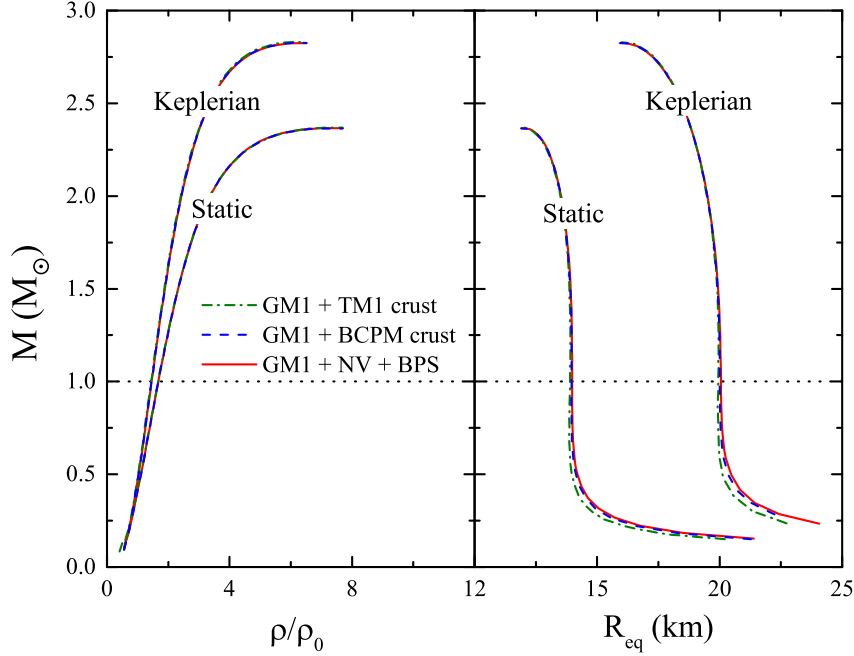


**Figure 3.** (Color online) NSs’ masses as functions of central density (left panel) and radius (right panel) for three cases of crust EoSs (Shen-TM1, BCPM, NV + BPS) matching with one GM1 core EoS, with the detailed EoS matching data shown in Table 1. The calculations are done for both static case and Keplerian rotating case. See text for details.

While  $(n_0, E/A)$  are very similar for all core EoS models, relatively large differences are present in the two RMF EoSs for  $(K, E_{\text{sym}}, L)$ , and they are usually larger than the current empirical values, which are listed in the last row. However, as we will see later, these rather big differences in  $(K, E_{\text{sym}}, L)$  will result in insignificant effects on the star mass and/or radius for NSs with  $M > 1.0M_{\odot}$ .

The crust effects on the star’s mass-radius relations in non-unified EoSs are shown in Fig. 3, where three widely-used crust EoSs (Shen-TM1, BCPM, NV + BPS) are matched with one core EoS (GM1). Using tabulated EoS, we compute stationary and equilibrium sequences of rapidly rotating, relativistic stars in general relativity from the well-tested *rns* code (<http://www.gravity.phys.uwm.edu/rns/>), assuming the matter comprising the star to be a perfect fluid. More details about the code can be found in, e.g., Refs. [52, 53, 54]. It is clear that for both static case and Keplerian rotating case, the results hardly depend on how the inner crusts are described. This is true not only for the maximum mass and central densities, but also for the radii. For less massive stars, the crust-core matching has relatively larger effects on the radii, and the TM1 curves (green ones in the right panel) deviate a little from the other two, due to relatively larger difference in the crust-core interface for Shen-TM1 mentioned before.

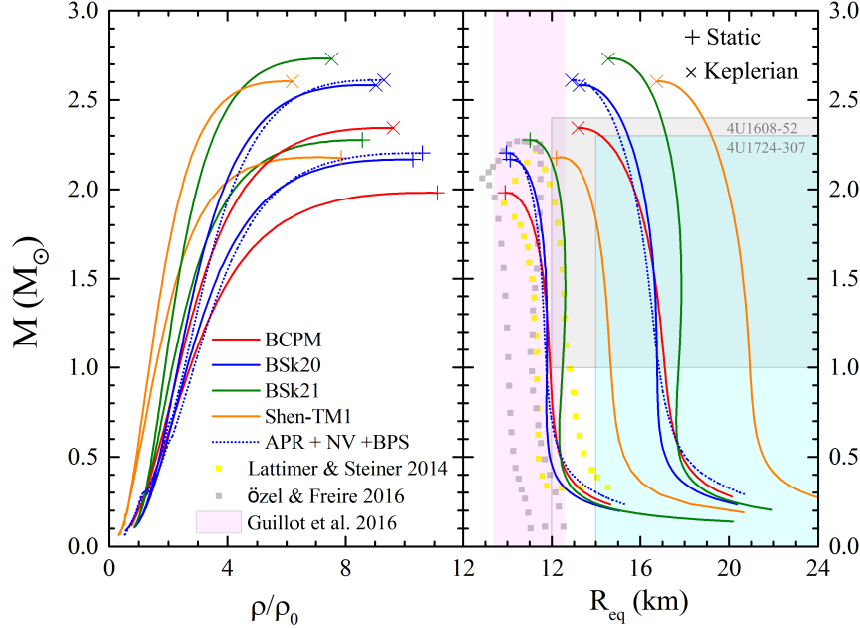


**Figure 4.** (Color online) NSs’ masses as functions of central density (left panel) and radius (right panel) for four unified EoSs (BCPM, BSk20, BSk21, Shen-TM1) in solid lines. The results from one representative non-unified EoS (APR + NV + BPS) is also shown in dashed lines for comparing with the BSk20 ones. The calculations are done for both static case (with plus signs labelling the corresponding maximum masses) and Keplerian rotating case (with cross signs labelling the corresponding maximum mass). Three recent radius determinations (Lattimer & Steiner 2014, Özel & Freire 2016, Guillot et al. 2016) are also shown, as well as those of two X-ray sources in low-mass X-ray binaries (4U1724-307, 4U1608-52). See text for details.

This deviation may be relevant only for NSs’ masses smaller than  $1.0M_{\odot}$  [12].

A complete set of results is shown in Fig. 4 and Table 3. It is clear that rotation increases both the gravitational mass and the radius, and at the same time it lowers the central density from  $\sim 7 - 10\rho_0$  to  $\sim 6 - 9\rho_0$ . Possible highest spin frequencies  $f_K$  are all higher than 1000 Hz, while the current observed maximum is  $f = 716$  Hz [55] for PSR J1748-2446a in the globular cluster Terzan 5. A possible reason for this discrepancy is that the star fluid is suffering from r-mode instability. A simple estimation showed that this would lower the maximum frequency by  $\sim 37\%$  [56], which would satisfactorily explain the observations up to date. In particular, rotation can increase the star’s gravitational mass up to  $\sim 18\% - 19\%$ , and the star can be as massive as  $\sim 2.7 M_{\odot}$  in the BSk21 case. Also, the star becomes flattened and the corresponding circumferential radius is increased up to  $\sim 3 - 4$  km, i.e.  $\sim 29\% - 36\%$ . For less heavy star like  $1.4 M_{\odot}$ , the radius increase is more pronounced, reaching  $\sim 5 - 6$  km, i.e.  $\sim 41\% - 43\%$ .

In Fig. 4, right panel, recent radius determinations [57, 58] are also shown in scattered areas, as well as the updated results from surface thermal emission of quiescent

**Table 3.** Static ( $f = 0$ ) and maximally spinning ( $f = f_K$ , labelled by the superscript K) configurations for employed EoSs, for maximum-mass stars (in the 3<sup>rd</sup> – 10<sup>th</sup> columns) and  $1.4M_\odot$  stars (in the last three columns). The spin frequency  $f_K$  is in Hz, the central energy density ( $\rho_c, \rho_c^K$ ) is in  $\rho_0$ , the maximum gravitational mass ( $M_{\max}, M_{\max}^K$ ) in  $M_\odot$ , and the radii ( $R_{\text{eq,max}}, R_{\text{eq,max}}^K, R_{\text{eq,max}}^{(1.4)}, R_{\text{eq,max}}^{(1.4),K}$ ) in km. The percent in the 7<sup>th</sup>, 10<sup>th</sup>, 13<sup>th</sup> columns are the corresponding relative increases by Keplerian rotating.

EoS	$f_K$ (Hz)	$\rho_c$ ( $\rho_0$ )	$\rho_c^K$ ( $\rho_0$ )	$M_{\max}$ ( $M_\odot$ )	$M_{\max}^K$ ( $M_\odot$ )	percent /	$R_{\text{eq,max}}$ (km)	$R_{\text{eq,max}}^K$ (km)	percent /	$R_{\text{eq,max}}^{(1.4)}$ (km)	$R_{\text{eq,max}}^{(1.4),K}$ (km)	percent /
BCPM	1791	10.9	9.44	1.98	2.34	18.2	9.94	13.24	33.2	11.71	16.76	43.1
BSk20	1855	10.0	8.80	2.17	2.58	18.9	10.17	13.32	31.0	11.76	16.67	41.8
APR*	1940	10.1	9.16	2.20	2.61	18.6	10.04	12.95	29.0	11.59	16.45	41.9
BSk21	1661	8.35	7.34	2.28	2.73	19.7	11.08	14.65	32.2	12.60	17.85	41.7
Shen-TM1	1333	7.08	5.94	2.18	2.60	19.3	12.40	16.88	36.1	14.45	20.72	43.4

LMXBs inside globular clusters, namely  $10.8_{-1.4}^{+1.8}$  km [59]. We see that all EoS except the Shen-TM1 are in agreement with all three current radius determinations. We notice that large NS radii have been determined from the photospheric radius expansion (PRE) burst in 4U 1724-307 ( $> 14$  km for  $M < 2.3M_\odot$ ) and X-ray buster in 4U 1608-52 ( $> 12$  km for  $1 \leq M \leq 2.4M_\odot$ ). As seen in the shaded area in Fig. 4, nearly all accurate static calculations from various present EoS can not reconcile the observations of these two pulsars, and this confirms the argument that a high spin might play a role in the observed large radii for both objects. This is because rotation at a known spin at 620 Hz ( $\sim 35\%$  for the BCPM EoS) may easily have a  $> 10\%$  larger radius in 4U 1608-52, and this would be consistent with the observations.

### 3. Conclusions

In the present work we aim to study how the (inner) crust EoS in non-unified EoSs affects the stars' rotating configurations as rapidly as the Keplerian limit, and also try to provide quantitative results for fast-rotating NSs.

For this purpose, four recently constructed unified EoSs, namely BCPM, BSk20, BSk21, Shen-TM1, are employed to perform calculations on the fast rotating configurations based on the *rns* code. The widely-used BPS outer crust EoS and the NV inner crust EoS are also used for comparison, as well as the APR and GM1 core EoS. All the core EoS chosen here satisfy the recent observational constraints of the two massive pulsars whose masses are precisely measured.

As far as the effects of the crust is concerning, we find that a non-smooth matching interface between core and inner crust produces a slight deviation in the mass-radius relation with respect to the unified description, even for the maximally-spinning (Keplerian) rotating configuration. Those small changes are visible for star masses



less than  $1M_{\odot}$ , in agreement with previously findings [12]. For all four unified EoSs, rotation can increase the star's gravitational mass up to  $\sim 19\%$ , and the corresponding circumferential radius up to  $\sim 36\%$ , depending on the core EoS. For stars as heavy as  $1.4 M_{\odot}$ , the radius increase may reach up to  $\sim 5 - 6\text{km}$ . Moreover, by confronting the present calculations with recent simultaneous determinations of mass and radius for two X-ray bursts 4U 1608-52 and 4U 1724-307, we address that they are possibly NSs that are spinning rapidly, in order to account for the measured large radii.

In terms of future methods, useful constrains could be possible by combining gravitational wave and electromagnetic observations from both coalescing NS-NS binaries and isolated NSs. It would be interesting and meaningful to study whether NS EoS could be determined from gravitational wave emission from elliptically deformed pulsars [60] and NS-NS binaries [11].

#### 4. Acknowledgements

We would like to thank Hong Shen, Guo-Yun Shao, and Xia Zhou for valuable discussions. The work was supported by the National Natural Science Foundation of China (No 11675094 and No U1431107).

#### 5. References

- [1] Ray P S, Philips B F, Wood K S, Chakrabarty D, Remillard R A, Wilson-Hodge C A 2011 arXiv: 1109.1309
- [2] Nan R D *et al* 2011 *Int. J. Mod. Phys. D* **20** 989
- [3] Gendreau K C, Arzoumanian Z, Oka jima T 2012 *Proceedings of the SPIE* **8443** 844313
- [4] Feroci M *et al* *Experimental Astronomy* 2012 **34** 415
- [5] Zhang S N *et al* 2016 arXiv:1607.08823
- [6] Suleimanov V F, Poutanen J, Klochkov D and Werner K 2016 *Eur. Phys. J. A* **52** 20
- [7] Miller M C and Lamb F K 2016 *Eur. Phys. J. A* **52** 63
- [8] Fortin M, Providencia C, Raduta A R, Gulminelli F, Zdunik J L, Haensel P and Bejger M, arXiv:1604.01944
- [9] Pais H, Menezes D P and Providência C 2016 *Phys. Rev. C* **93** 065805
- [10] Li A, Dong J M, Wang J B and Xu R X 2016 *ApJS* **223** 16
- [11] Li A, Zhang B, Zhang N B, Gao H, Qi B and Liu T 2016 arXiv: 1606.02934
- [12] Baldo M, Burgio G F, Centelles M, Sharma B K and Vinas X 2014 *Phys. At. Nucl.* **77** 1157
- [13] Stergioulas N 2003 *Living Rev. Relat.* **6** 3
- [14] Qi B *et al.* 2016 *Res. Astron. Astrophys.* **16** 60
- [15] Demorest P B, Pennucci R, Ransom S M, Roberts M S E and Hessels J W T 2010 *Nature* **467** 1081
- [16] Antoniadis J, *et al.* 2013 *Science* **340** 6131
- [17] Fonseca E *et al* arXiv:1603.00545
- [18] Sharma B K, Centelles M, Vinas X, Baldo M and Burgio G F 2015 *Astron. Astrophys.* **584** A103
- [19] Potekhin A Y, Fantina A F, Chamel N, Pearson J M and Goriely S 2013 *Astron. Astrophys.* **560** A48
- [20] Shen H, Toki H, Oyamatsu K and Sumiyoshi K 1998 *Nucl. Phys. A* **637** 435
- [21] Akmal A, Pandharipande, V R and Ravenhall D G 1998 *Phys. Rev. C* **58** 1804
- [22] Glendenning N K and Moszkowski S A 1991 *Phys. Rev. Lett.* **67** 241
- [23] Baym G, Pethick C and Sutherland D 1971 *ApJ* **170** 299

- [24] Negele J W and Vautherin D 1973 *Nucl. Phys.* **A207** 298
- [25] Baldo M 1999 *Nuclear Methods and the Nuclear Equation of State*, ed. M. Baldo (Singapore: World Scientific), 1
- [26] Haensel P, Bejger M, Fortin M, Zdunik L 2016 arXiv: 1601.05368
- [27] Morrison I A, Baumgarte T W, Shapiro S L and Pandharipande V R 2004 *ApJ* **617** L135
- [28] Lattimer J M and Schutz B F 2005 *ApJ* **629** 979
- [29] Zheng X P, Pan N N, Zhang L 2007 arXiv: 0712.4310
- [30] Worley A, Krastev P G and Li B A 2008 *ApJ* **685** 390
- [31] Read J S, Lackey B D, Owen B J and Friedman J L 2009 *Phys. Rev. D* **79** 124032
- [32] Urbanec M, Miller J C and Stuchlik Z 2013 *Mon. Not. R. Astron. Soc.* **433** 1903
- [33] Steiner A W, Gandolfi S, Fattoyev F J and Newton W G 2015 *Phys. Rev. C* **91** 015804
- [34] Li A, Wang J B, Shao L J and Xu R X 2015 *Acta Astronom. Sin. Suppl.* **56** 22
- [35] Li A, Wang J B, Shao L J and Xu R, X 2016 arXiv: 1601.05368
- [36] Bhattacharyya S, Bombaci I, Logoteta D and Thampan A V 2016 *Mon. Not. R. Astron. Soc.* **457** 3101
- [37] Suleimanov V, Poutanen J, Revnivtsev M and Werner K 2011 *ApJ* **742** 122
- [38] Poutanen J et al 2014 *Mon. Not. R. Astron. Soc.* **442** 3777
- [39] Link B, Epstein R I and Lattimer J M 1999 *Phys. Rev. Lett.* **83** 3362
- [40] Andersson N, Glampedakis K, Ho W C and Espinoza C M 2012 *Phys. Rev. Lett.* **109** 241103
- [41] Chamel N 2013 *Phys. Rev. Lett.* **110** 011101
- [42] Piekarewicz J, Fattoyev F J and Horowitz C J 2014 *Phys. Rev. C* **90** 015803
- [43] Li A 2015 *Chinese Phys. Lett.* **32** 079701
- [44] Burgio G F, Schulze H-J and Li A 2011 *Phys. Rev. C* **83** 025804
- [45] Hu J N, Li A, Toki H and Zuo W 2014 *Phys. Rev. C* **89** 025802
- [46] Zuo W, Li A, Li Z H and Lombardo U 2004 *Phys. Rev. C* **70** 055802
- [47] Li A, Burgio G F, Lombardo U and Zuo W 2006 *Phys. Rev. C* **74** 055801
- [48] Li A, Zhou X R, Burgio G F and Schulze H J 2010 *Phys. Rev. C*, **81** 025806
- [49] Zhu Z Y, Li A, Hu J N and Sagawa H 2016 *Phys. Rev. C* **94** 045803
- [50] Peng G X, Li A and Lombardo U 2008 *Phys. Rev. C* **77** 065807
- [51] Li A, Zuo W and Peng G X 2015 *Phys. Rev. C* **91** 035803
- [52] Komatsu H, Eriguchi Y and Hachisu I 1989 *Mon. Not. R. Astron. Soc.* **237** 355
- [53] Cook G B, Shapiro S L and Teukolsky S A 1994 *ApJ* **422** 227
- [54] Stergioulas N and Friedman J L 1995 *ApJ* **444** 306
- [55] Hessels J W T, Ransom S M, Stairs I H, et al 2006 *Science* **311** 1901
- [56] Li A, Zhou X et al 2016 in preparation
- [57] Lattimer and Steiner 2014 *Eur. Phys. J. A* **50** 40
- [58] Ozel and Freire 2016 *Annu. Rev. Astron. Astrophys* **54** 401
- [59] Guillot S et al private communication and in preparation
- [60] Krastev P G and Li B A 2016 arXiv:1607.05373